Measuring the fine-structure constant to refine the Standard Model predictions

Saïda Guellati-Khélifa

Short story of the fine-structure contant

$$\alpha = \frac{e^2}{4\pi\epsilon_0\hbar c} \sim \frac{1}{137}$$

- Sommerfeld-Bohr model = elliptical orbits+ relativistic mass +…
  To explain the splitting of Balmer lines in hydrogen spectrum (fine structure)

Für das *eigentliche Balmersche Wasserstoffspektrum* $(E = e)$ kann man etwas kürzer schreiben:

$$(18\,\mathrm{a}) \qquad \left\{ \begin{aligned} \nu = \frac{m_0\,c^2}{h} \Bigg(& \left(1 + \frac{\alpha^2}{(n' + \sqrt{n^2 - \alpha^2})^2}\right)^{-1/2} \\ & - \left(1 + \frac{\alpha^2}{(m' + \sqrt{m^2 - \alpha^2})^2}\right)^{-1/2} \Bigg). \end{aligned} \right.$$

A. Sommerfeld, Annalen der Physik 51, 1-94, 125-167 (1916)

- First precise determination of the fine-structure constant $\frac{\sigma_\alpha}{\alpha} \simeq 0.004$

Short story of the fine-structure contant

1928, Dirac equation

- Energy levels of hydrogen atom: $E(n,j) \simeq m_e c^2 \left[1 - \frac{\alpha^2}{2n^2} - \frac{\alpha^4}{2n^4}\left(\frac{n}{j+\frac{1}{2}} - \frac{3}{4}\right) + ...\right]$

  $\longrightarrow hcR_\infty = \frac{1}{2} m_e \alpha^2 c^2$

- Electron magnetic moment: $\vec{\mu}_e = -g_e \frac{e}{2m_e}\vec{S}, \quad g_e = 2$

- Prediction of anti-particles, positron observed by C. D. Anderson in 1932.

- Lamb–Retherford experiment: 1050 MHz energy shift between $^2S_{1/2}$ and $^2P_{1/2}$ hydrogen levels

  W. E. Lamb, and R. C. Retherford , Phys. Rev. 72, 1256 (1947)

- Measurement of *g*-factors of Ga, In and Na: $\Longrightarrow g_e = 2.00229 \pm 0.00008$

  P. Kush and H. M. Foley, Phys. Rev. 72, 1256 (1947)

Corrections due to the coupling with quantum vacuum ⟶ Birth of quantum electrodynamics

Anomalous Magnetic Moment of the Electron: QED contributions

- Vacuum fluctuations and polarization modify the interaction of the electron with the magnetic field,

$$a_e = \frac{g_e - 2}{2} \simeq \frac{1}{2}\frac{\alpha}{\pi}$$

Schwinger, Phys. Rev. 73, 416 (1948); Phys. Rev. 75, 898 (1949)

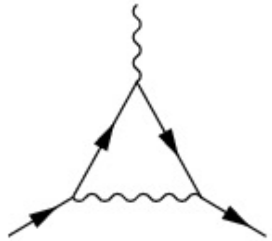

Feynman diagram for the one photon-loop correction for the free electron

- Higher order corrections: perturbative series of $\alpha = 1/137.036 \approx 0.007$

J. Schwinger, R. Feynman, E. Stueckelberg, S. Tomonaga....

$$a_e(\mathrm{QED}) = \underbrace{A_1}_{e,\gamma} + \underbrace{A_2(m_e/m_\mu)}_{e,\mu,\gamma} + \underbrace{A_2(m_e/m_\tau)}_{e,\tau,\gamma} + \underbrace{A_3(m_e/m_\mu, m_e/m_\tau)}_{e,\mu,\tau,\gamma}$$

$$A_i = A_i^{(2)}\left(\frac{\alpha}{\pi}\right) + A_i^{(4)}\left(\frac{\alpha}{\pi}\right)^2 + A_i^{(6)}\left(\frac{\alpha}{\pi}\right)^3 + A_i^{(8)}\left(\frac{\alpha}{\pi}\right)^4 + \cdots$$

QED contribution: 8th order term

- 891 Feynman diagrams contribute to 8th order $A_1^{(8)}$ term.

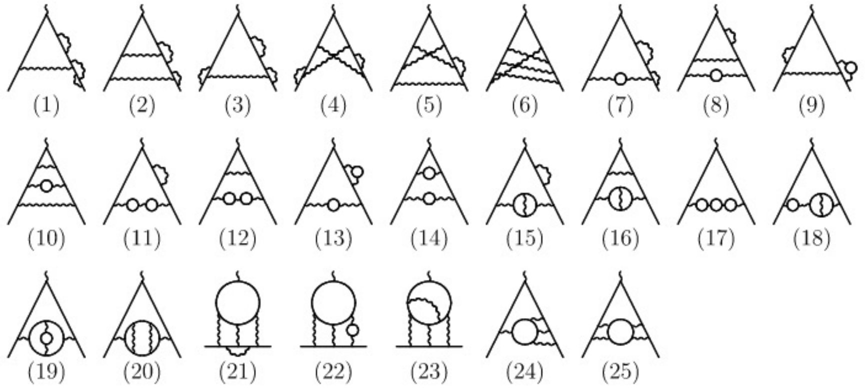

Standard model prediction of a_e

Coefficient $A_i^{(2n)}$	Value (Error)	References	
$A_1^{(2)}$	0.5	Schwinger 1948	
$A_1^{(4)}$	$-0.328\,478\,965\,579\,193\cdots$	Petermann 1957, Sommerfield 1958	
$A_2^{(4)}(m_e/m_\mu)$	$0.519\,738\,676\,(24)\times10^{-6}$	Elend 1966	
$A_2^{(4)}(m_e/m_\tau)$	$0.183\,790\,(25)\times10^{-8}$	Elend 1966	
$A_1^{(6)}$	$1.181\,241\,456\,587\cdots$	Laporta-Remiddi 1996, Kinoshita 1995	
$A_2^{(6)}(m_e/m_\mu)$	$-0.737\,394\,164\,(24)\times10^{-5}$	Samuel-Li, Laporta-Remiddi, Laporta	72 diagrams
$A_2^{(6)}(m_e/m_\tau)$	$-0.658\,273\,(79)\times10^{-7}$	Samuel-Li, Laporta-Remiddi, Laporta	
$A_3^{(6)}(m_e/m_\mu, m_e/m_\tau)$	$0.1909\,(1)\times10^{-12}$	Passera 2007	
$A_1^{(8)}$	$-1.912\,245\,764\cdots$	Laporta 2017, AHKN 2015	
$A_2^{(8)}(m_e/m_\mu)$	$0.916\,197\,070\,(37)\times10^{-3}$	Kurz et al 2014, AHKN 2012	
$A_2^{(8)}(m_e/m_\tau)$	$0.742\,92\,(12)\times10^{-5}$	Kurz et al 2014, AHKN 2012	891 diagrams
$A_3^{(8)}(m_e/m_\mu, m_e/m_\tau)$	$0.746\,87\,(28)\times10^{-6}$	Kurz et al 2014, AHKN 2012	
$A_1^{(10)}$	6.737 (159)	AKN 2018,2019	
$A_2^{(10)}(m_e/m_\mu)$	$-0.003\,82\,(39)$	AHKN 2012,2015	
$A_2^{(10)}(m_e/m_\tau)$	$\mathcal{O}(10^{-5})$		12671 diagrams
$A_3^{(10)}(m_e/m_\mu, m_e/m_\tau)$	$\mathcal{O}(10^{-5})$		

- T. Aoyama, T. Kinoshita, M. Nio, Phys. Rev. D 2018, 97, 036001.
- S. Laporta, Phys. Lett. B 2017, 772, 232–238.
- T. Aoyama, T. Kinoshita and M. Nio, Atoms 2019, 7, 28
- R. Bouchendira et al., Phys. Rev. Lett. 2011, 106, 080801.
- R.H. Parker et al, Science 2018, 360, 191–195.

$$a_e(\text{theo}) = a_e(\text{QED}) + a_e(\text{Hadron}) + a_e(\text{Weak})$$

$$a_e(\text{theory}:\alpha(\text{Rb})) = 1159652182.037\,(720)\,(11)\,(12)\times10^{-12}$$

$$a_e(\text{theory}:\alpha(\text{Cs})) = 1159652181.606\,(229)\,(11)\,(12)\times10^{-12}$$

(12) → hadronic contribution

(11) → Numerical evaluation of the tenth-order QED

(720), (229) → Fine-structure constant

Measurement of the anomalous magnetic moment of the electron

R. S. Van Dyck., P. B. Schwinberg and H. G. Dehmelt. Phys. Rev. D 34, 722 (1986) and Phys. Rev. Lett. 59, 26 (1987)

- Electron in a magnetic field

$$\frac{g_\mathrm{e}}{2} = \left|\frac{\mu_\mathrm{e}}{\mu_\mathrm{B}}\right| = \frac{\nu_\mathrm{s}}{\nu_\mathrm{c}} = 1 + \frac{\nu_\mathrm{s}-\nu_\mathrm{c}}{\nu_\mathrm{c}} = 1 + \frac{\nu_\mathrm{a}}{\nu_\mathrm{c}}$$

$$\mu_\mathrm{B} = \frac{e}{2m_\mathrm{e}\hbar} \text{ : Bohr magneton}$$

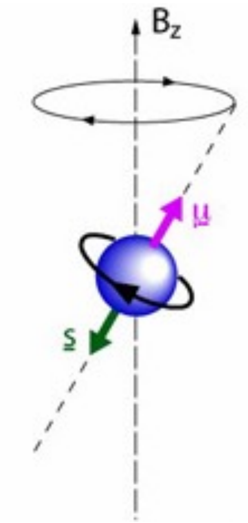

$$E_{n,m_\mathrm{s}} = m_s h\nu_\mathrm{s} + \left(n+\frac{1}{2}\right)h\nu_\mathrm{c}$$

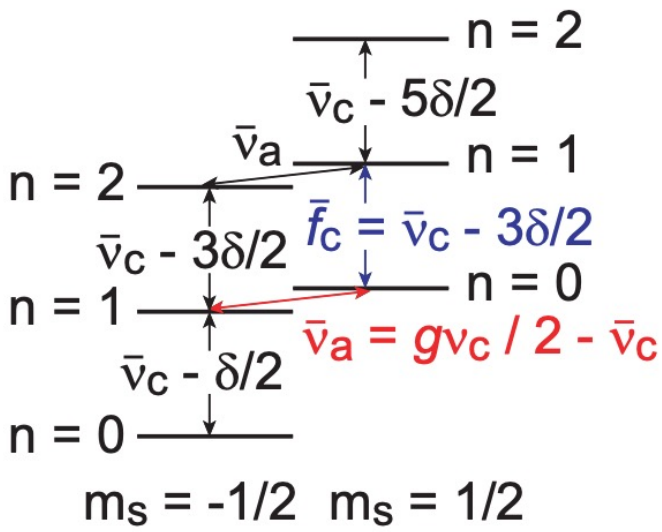

Advantages

- The magnetic field dependence drops out of the ratio.
- ν_c and ν_s differs by 10^{-3}, measuring frequencies to $10^{-10} \longrightarrow g_e$ to 10^{-13}

Measurement of the electron magnetic moment: Harvard experiment

Hanneke, D.; Fogwell, S.; Gabrielse, G. Phys. Rev. Lett. 2008, 100, 120801.

- Electron in Penning trap + magnetic field

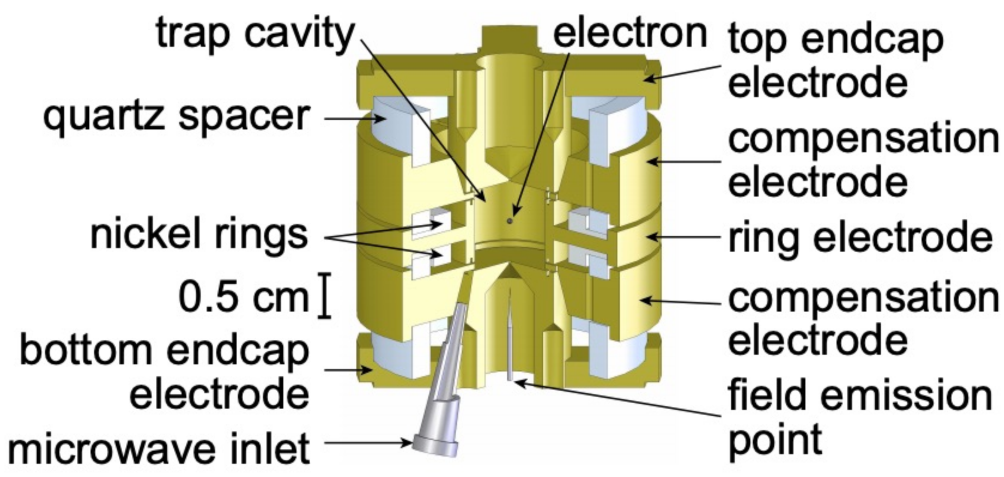

$$a_e(\exp) = \frac{g_e - 2}{2} = 0.00115965218073\ (28)\ [0.28\ \text{ppt}]$$

Quantum-jump spectroscopy

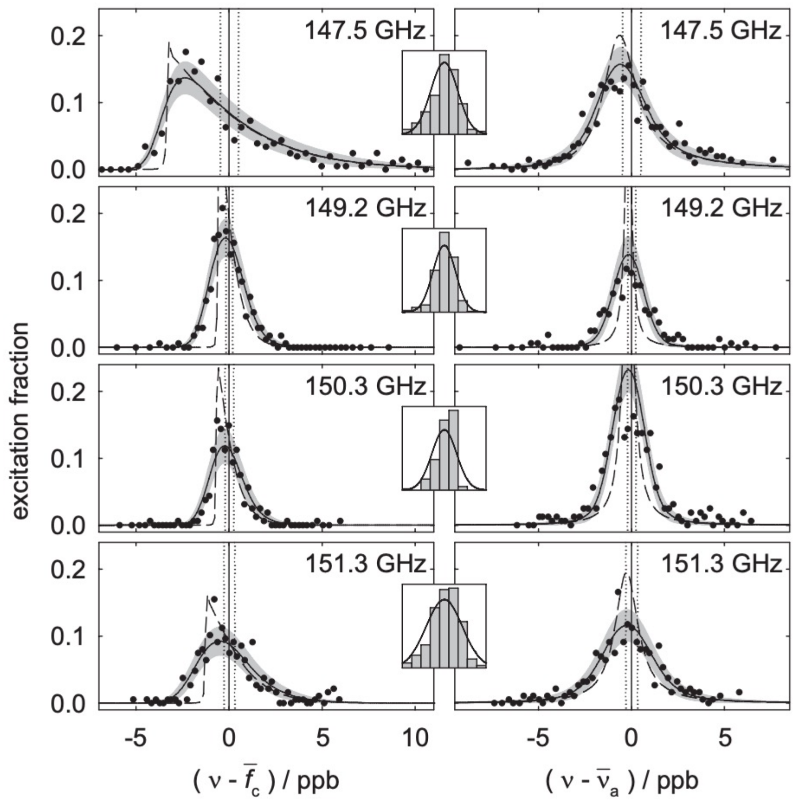

- 10 times improved accuracy is expected
  - New experimental setup (better control of the electron motion, reduction of magnetic field gradient)
  - The spin and cyclotron transition frequencies measured nearly simultaneously

X. Fan and G. Gabrielse, Phys. Rev. A 103, 022824 (2021)

Test of Quantum electrodynamics and Standard model

α : coupling constant of electromagnetic interaction

Transition frequencies measurement

Muonium ground-state hyperfine splitting

$$\Delta\nu_{\mathrm{Mu}}(\mathrm{th}) = \Delta\nu_F \times \mathcal{F}(\alpha, m_e/m_\mu)$$

$$\Delta\nu_F = \frac{16}{3} c R_\infty Z^3 \alpha^2 \frac{m_e}{m_\mu}\left(1+\frac{m_e}{m_\mu}\right)^{-3}$$

Anomalous Magnetic Moment of the Electron

$$a_e(\mathrm{theo}) \equiv a_e(\mathrm{exp})$$

Quantum Hall effect

$$R_K = \frac{h}{e^2} = \frac{\mu_0 c}{2\alpha}$$

Recoil measurement

$$\alpha^2 = \frac{2R_\infty}{c}\frac{m_{\mathrm{At}}}{m_e}\frac{h}{m_{\mathrm{At}}}$$

Paris, Berkeley

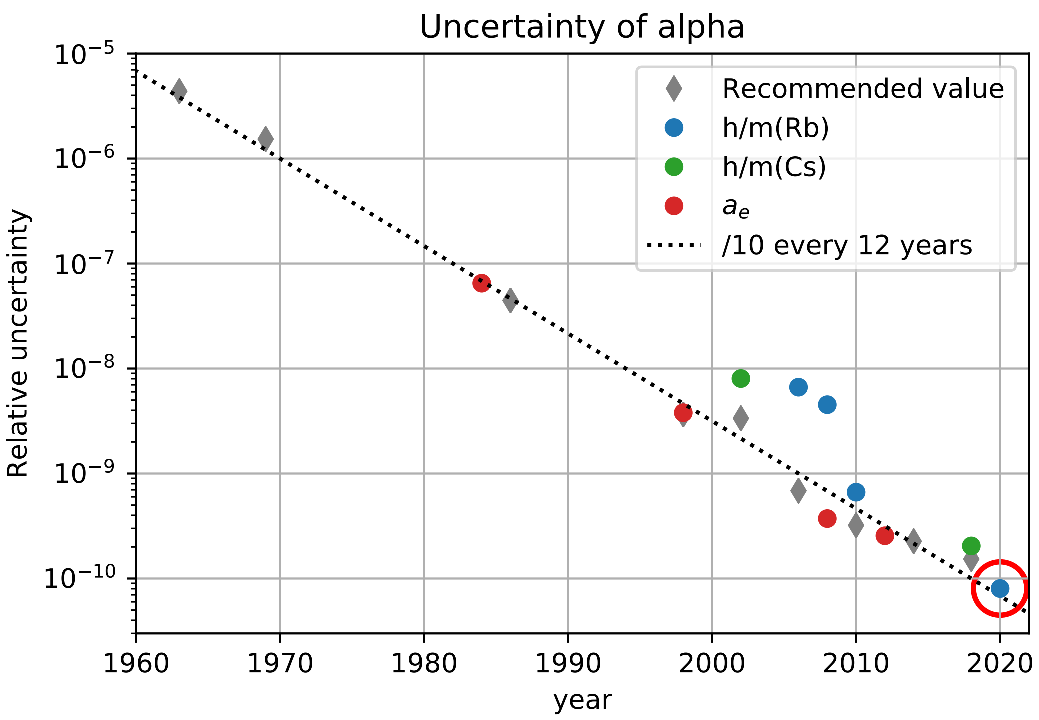

Physics beyond Standard Model ?

$$a_e(\mathrm{theo}) - a_e(\mathrm{exp}) \overset{?}{=} \delta a_e(\mathrm{BSM})$$

Outline

- Measurement of the ratio *h*/*M*
- Impact of the new determination of the fine-structure constant

Outline

- Measurement of the ratio h/M
- Impact of the new determination of the fine-structure constant

Recoil velocity

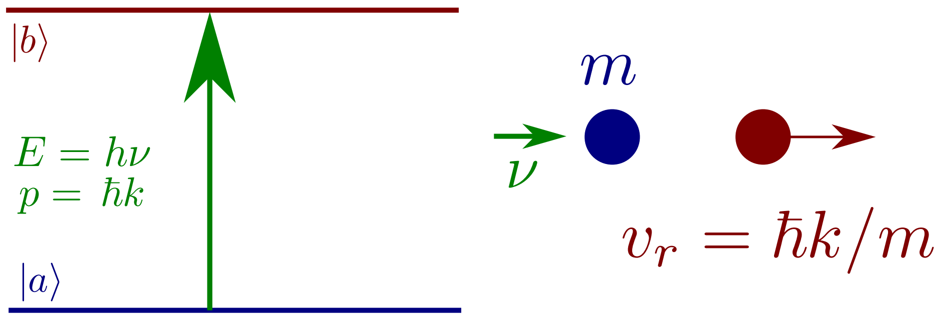

- v_r = 6 mm/s for Rb atom (for λ = 780 nm)
- Plane wave

$$v_{\mathrm{r}} = \frac{h}{m}\frac{1}{\lambda}$$

The ratio *h*/*m* and the fine-structure constant

- The Rydberg constant R_∞

$$hcR_\infty = \frac{1}{2} m_e \alpha^2 c^2 \implies \alpha^2 = \frac{2R_\infty}{c} \frac{h}{m_e} \implies \alpha^2 = \frac{2R_\infty}{c} \frac{A_r(\mathrm{Rb})}{A_r(\mathrm{e})} \frac{h}{m_{\mathrm{Rb}}}$$

- Hydrogen spectroscopy $\implies$ determination of R_∞ with a relative uncertainty of 2×10^{-12}
- Determination of relative atomic masses : $A_r(X) = \frac{m_X}{m_u}$
  - Cyclotron frequencies $A_r(Rb)$ at 7.0×10^{-11}
  - Magnetic moment of a single electron bound to a carbon nucleus $A_r(e)$ at 2.9×10^{-11}

- The limiting factor is the ratio $\frac{h}{m_{Rb}}$

- G. Audi et al., 2014 Nuclear Data Sheets 120, 1-5 (2014)
- S. Sturm et al. Nature 506, 476-470 (2014),
- P. J. Mohr et al. Rev. Mod. Phys. 88, 035009 (2016).

Measurement of the recoil velocity

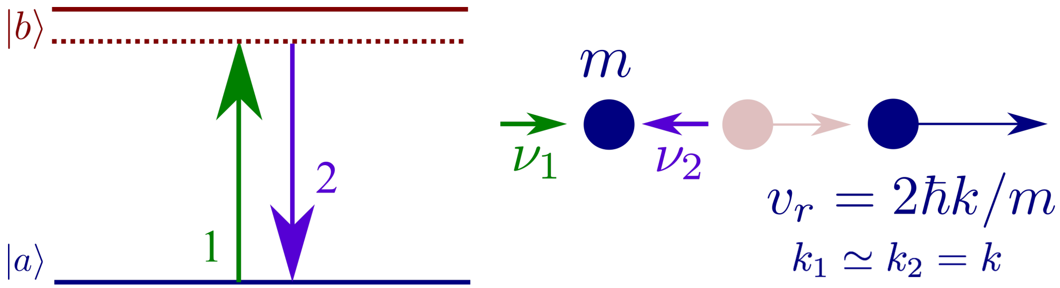

- Velocity sensor
  ⇒ Atom interferometer based on Raman transitions with a sensitivity: σ_v

- Transfer to atoms a large number *N* of photon momenta
  ⇒ Bloch oscillations technique

$$\sigma_{v_{\mathrm{r}}} = \frac{\sigma_v}{N}$$

Laboratoire Kastler Brossel
Physique quantique et applications

Basic concepts of atom interferometry

Matter waves

Louis De Broglie 1924

non - relativistic: $$\lambda_B = \frac{h}{mv}$$

For rubidium atom at $v = 6\ \mathrm{mm/s} \to \lambda_B \approx 7653\ \text{Å}$

Matter waves/cold atoms

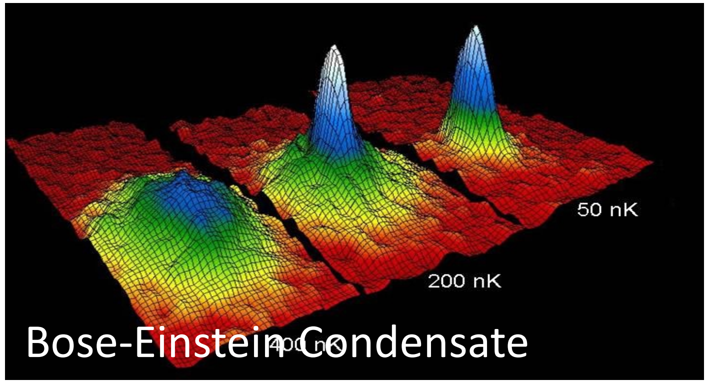

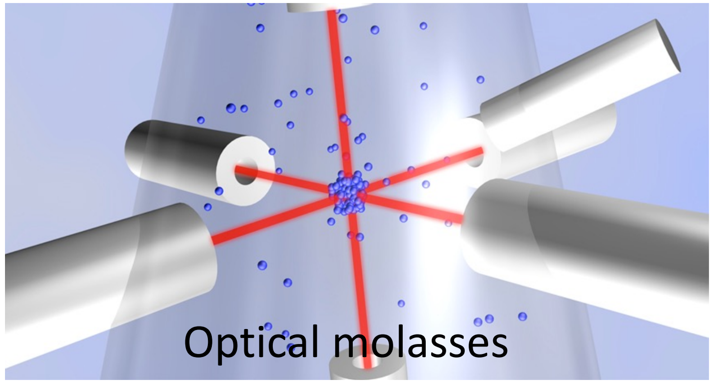

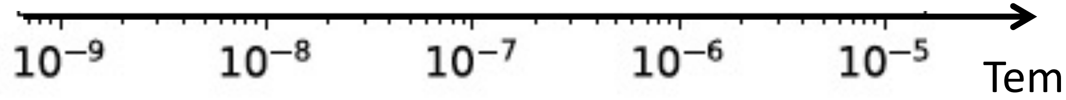

Coherence length: $\xi \sim \frac{\hbar}{\Delta p}$

Thermal De Broglie wavelength: $\lambda_T = \frac{h}{\sqrt{2\pi m k_B T}}$

To implement atomic interferometers for high-precision measurements, the challenge was to implement a technique for manipulating the matter waves in a coherent way

Atomic beamsplitter based on stimulated Raman transitions

$$\mathbf{E}_1(\mathbf{r},t) = \mathbf{E}_{01}\cos(\mathbf{k}_1\cdot\mathbf{r} - \omega_{L1}t + \phi_1)$$
$$\mathbf{E}_2(\mathbf{r},t) = \mathbf{E}_{02}\cos(\mathbf{k}_2\cdot\mathbf{r} - \omega_{L2}t + \phi_2)$$

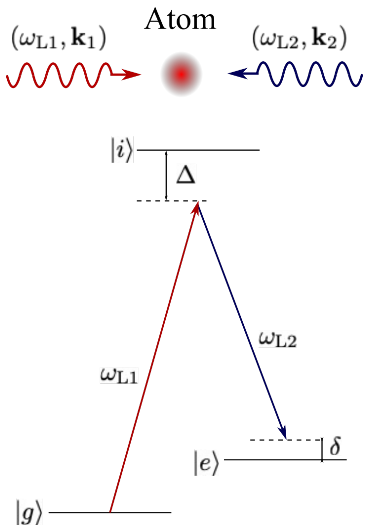

$\Delta \gg \delta$ and $\Delta \gg \Gamma$

at resonance

$$\Psi(0) = |g, \mathbf{p}_0\rangle$$
$$\Psi(t) = e^{-i\omega_1 t}\cos\left(\frac{\Omega t}{2}\right)|g,\mathbf{p}_0\rangle + e^{i\Delta\phi_L}e^{-i\omega_2 t}\sin\left(\frac{\Omega t}{2}\right)|e,\mathbf{p}_0 + \hbar\mathbf{k}_{\text{eff}}\rangle$$

The internal degrees of freedom are labelled by the external degrees

$\mathbf{k}_{\text{eff}} = \mathbf{k}_1 - \mathbf{k}_2$	effective wave vector
$\Delta\Phi_L$	Phase difference between the two lasers
Ω	Effective Rabi fréquence
$\omega_1 = \omega_g + \frac{\lvert\mathbf{p}\rvert^2}{2m}$	Energy in $\lvert g, \mathbf{p}\rangle$
$\omega_2 = \omega_e + \frac{\lvert\mathbf{p}+\hbar\mathbf{k}_{\text{eff}}\rvert^2}{2m}$	Energy in $\lvert e, \mathbf{p}+\hbar\mathbf{k}_{\text{eff}}\rangle$

Atomic beamsplitter based on stimulated Raman transitions

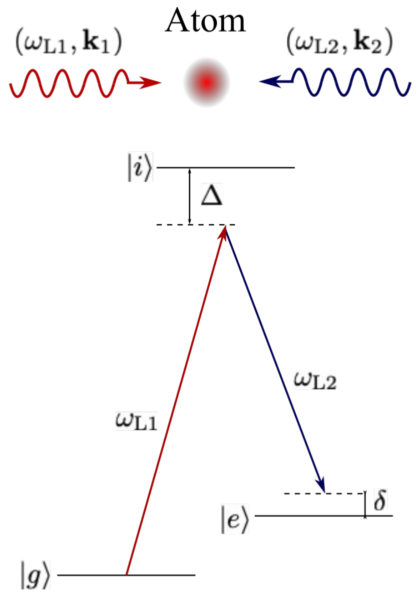

$$\Psi(t) = \mathrm{e}^{-i\omega_1 t} \cos\left(\frac{\Omega t}{2}\right) \; |g, \mathbf{p}_0\rangle + \mathrm{e}^{i\Delta\phi_L} \mathrm{e}^{-i\omega_2 t} \sin\left(\frac{\Omega t}{2}\right) \; |e, \mathbf{p}_0 + \hbar\mathbf{k}_{\mathrm{eff}}\rangle$$

$$\pi - \text{pulse} : \Omega\tau = \pi$$

$$\Psi(\tau) = \mathrm{e}^{i\Delta\phi_L} \mathrm{e}^{-i\omega_2 \tau} \; |e, \mathbf{p}_0 + \hbar\mathbf{k}_{\mathrm{eff}}\rangle$$

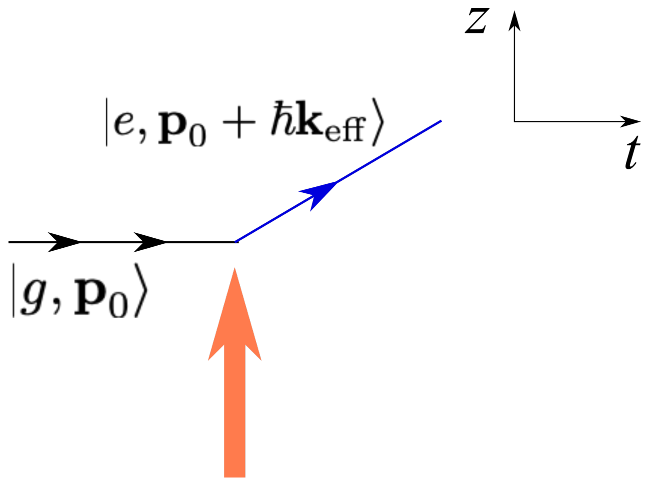

$$\frac{\pi}{2} - \text{pulse} : \Omega\tau = \frac{\pi}{2}$$

$$\Psi(\tau) = \frac{1}{\sqrt{2}} \left(\mathrm{e}^{-i\omega_1 \tau} \; |g, \mathbf{p}_0\rangle + \mathrm{e}^{i\Delta\phi_L} \mathrm{e}^{-i\omega_2 \tau} \; |e, \mathbf{p}_0 + \hbar\mathbf{k}_{\mathrm{eff}}\rangle\right)$$

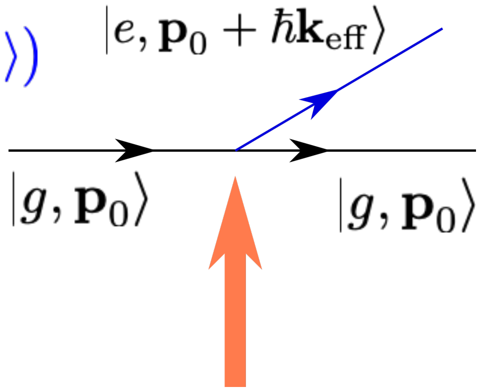

Phase shift of the atomic wave-packet along the propagating path

Laboratoire Kastler Brossel
Physique quantique et applications

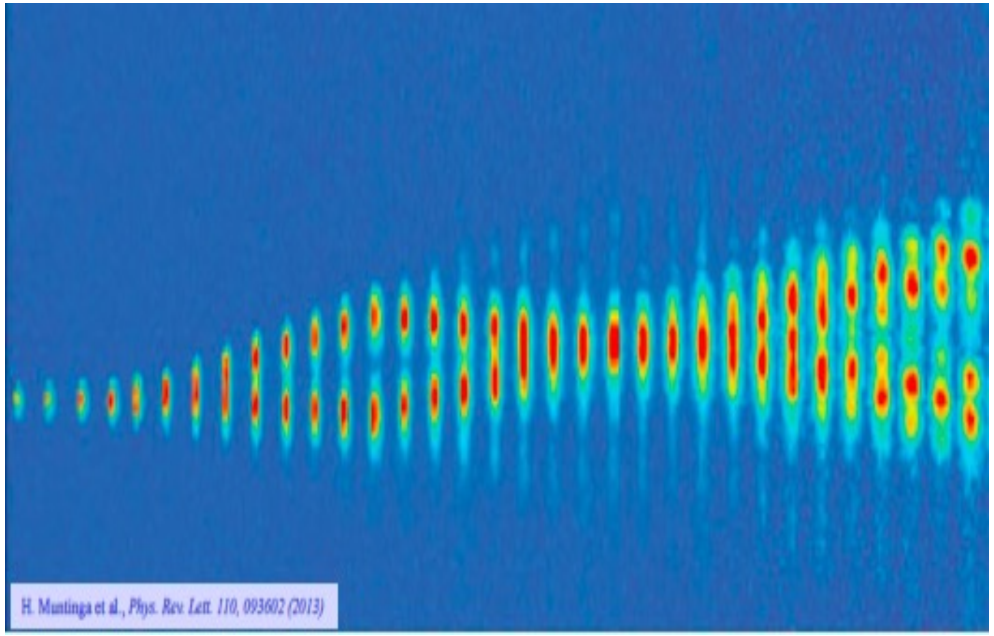

$$\phi_{\rm tot} = \phi_{\rm evol} + \phi_{\rm int} + \phi_{\rm sep}$$

Free evolution of wave-packets between light pulses

Phase due to atom-light interaction

Phase shift due to no overlap of the two arms at the last pulse

Luis De Broglie $\rightarrow$ phase of matter-wave $\psi = \exp -i\frac{mc^2}{\hbar}\tau$

Weak gravitational fields and velocities $\ll c$ $\quad d\tau \simeq dt - \frac{1}{mc^2}\mathcal{L}dt$

$$\psi(t) \simeq \exp\left[-i\frac{mc^2}{\hbar}t\right]\exp\left[\frac{i}{\hbar}\int\mathcal{L}dt\right] \qquad \phi_{\rm evol} = \frac{i}{\hbar}\int\mathcal{L}(z,t)dt$$

Mach Zehnder configuration: atom gravimeter

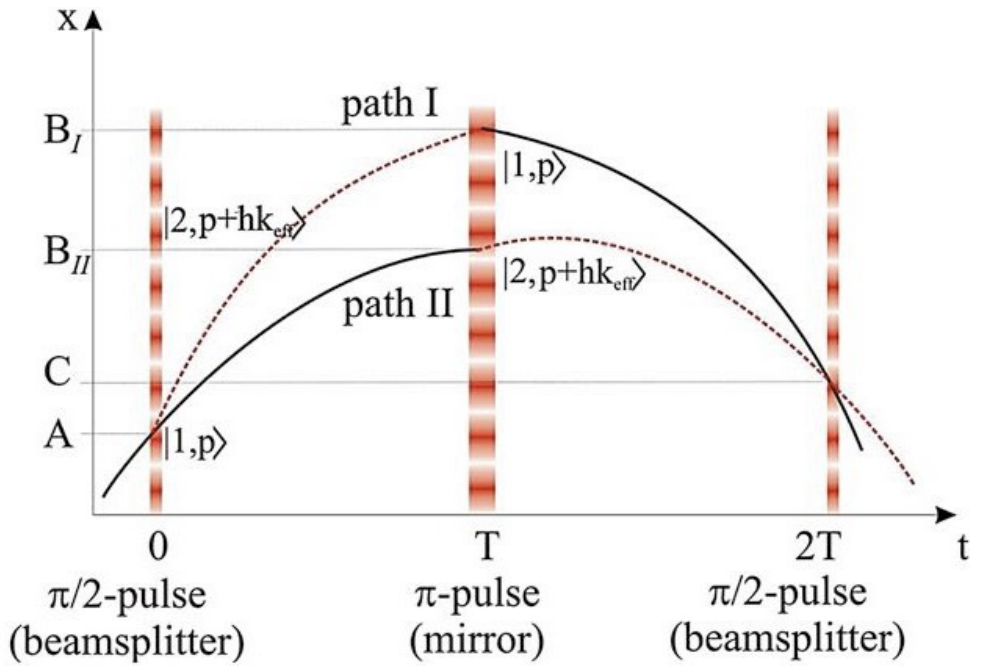

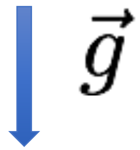

$$\phi_{\text{tot}} = k_{\text{eff}}\, g \left(T + \frac{4\tau}{\pi}\right)(T + 2\tau) + \delta\phi^0 \simeq k_{\text{eff}}\, g T^2$$

Velocity sensor: Ramsey-Bordé Atom interferometer

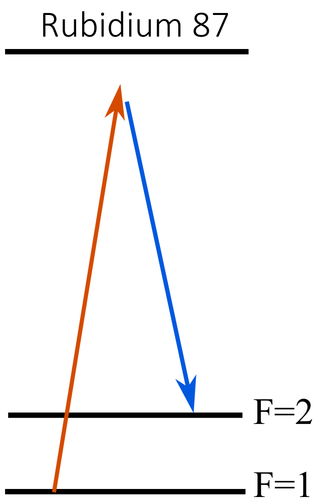

Free propagation: $e^{-i\omega_{1,2}t}$, $\omega_{1,2}$, depend on the kinetic energy

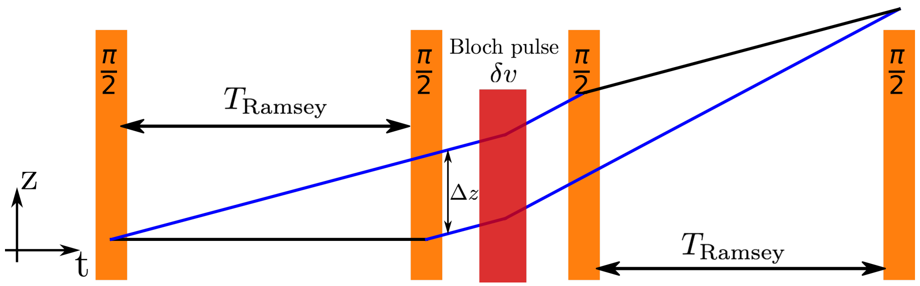

Probability to find an atom in $|2\rangle$

$$P_2 = \frac{1 + \cos\left(\Phi_{\text{at}} + \Phi_{\text{Las}}\right)}{2}$$

Velocity transfer δv

$$\Phi_{\text{at}} = T_{\text{Ramsey}} k_{\text{R}} \delta v = \frac{\Delta z \times m\delta v}{\hbar}$$

Sensitivity: $\delta z = 250\ \mu\text{m} \longrightarrow 3\ \mu\text{m} \cdot \text{s}^{-1} \cdot \text{rad}^{-1}$

Interferometer for the recoil measurement

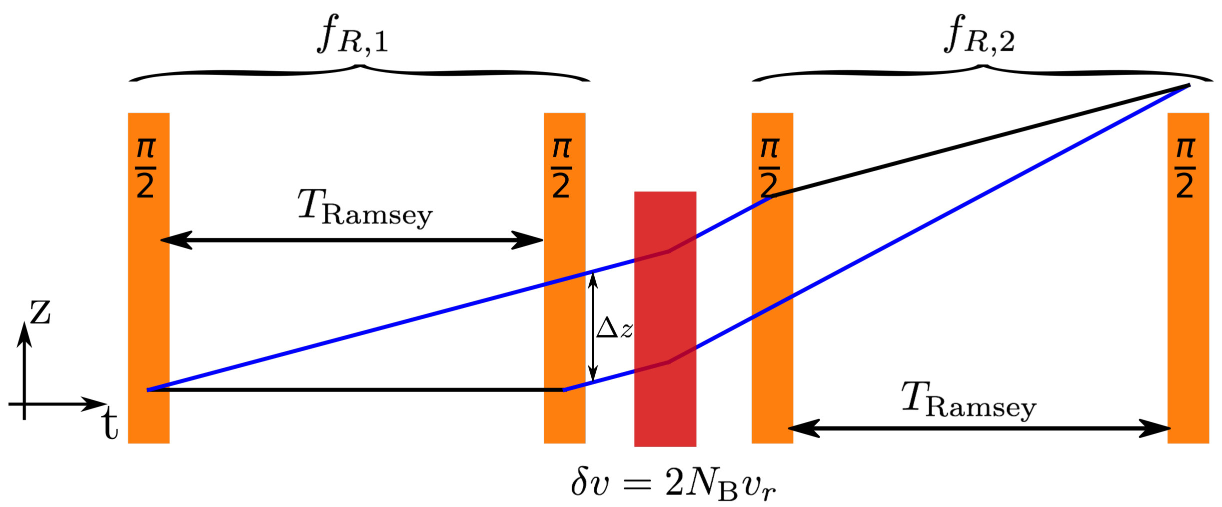

$$\Phi = T_{\rm Ramsey}\left(2N_B k_{\rm R} v_{\rm r} - 2\pi\delta f_{\rm R}\right)$$

$$\delta f_{\rm R} = f_{\rm R,2} - f_{\rm R,1}$$

Laboratoire Kastler Brossel
Physique quantique et applications

Coherent acceleration: Bloch oscillations technique

Coherent acceleration in optical lattice

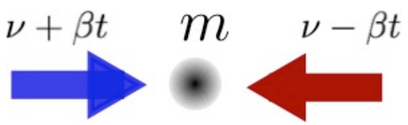

Succession of stimulated Raman transitions in the same internal level

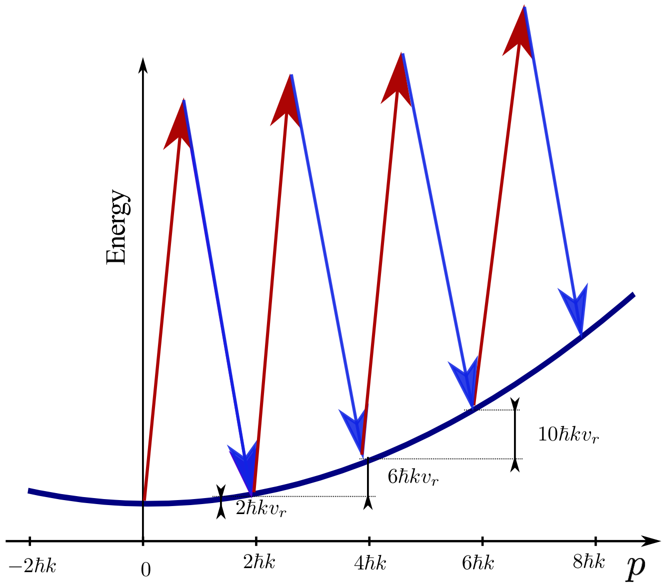

$$p_{\mathrm{in}} \rightarrow p_{\mathrm{in}} + 2N\hbar k$$

1000 photon momenta in 6 ms

- High momentum transfer efficiency: 99.95% per recoil
- Precise control of the velocity and the position of the atoms

Coherent acceleration: Bloch oscillations approach

(See Jean Dalibard lecture 2013)

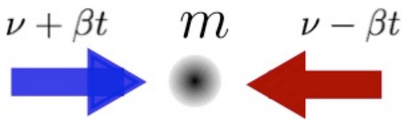

$V(x,t) = V_0 \sin^2\left(k\left(x - x_0(t)\right)\right); \quad x_0(t) = \lambda\beta t^2/2 = at^2/2$

accelerated frame

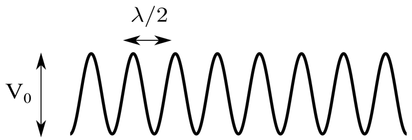

$+ \quad F = -m\ddot{x}_0(t) = -ma$

Adiabatic approximation

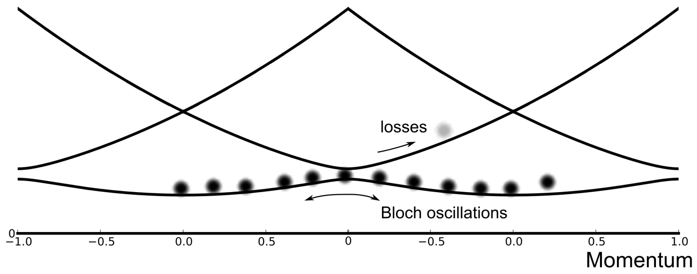

$$\text{Bloch oscillations period:} \quad \tau_B = \frac{2\hbar k}{a}$$

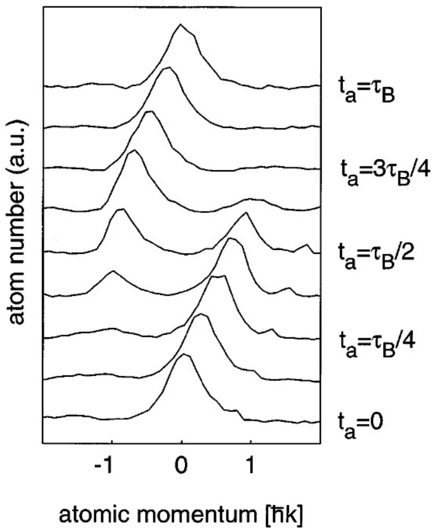

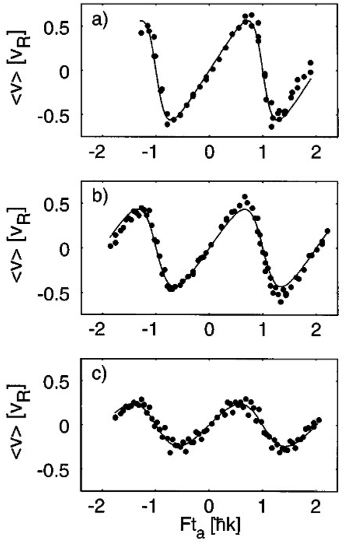

$p_{\text{in}}^{\text{Lab}} \rightarrow p_{\text{in}} + 2N\hbar k$

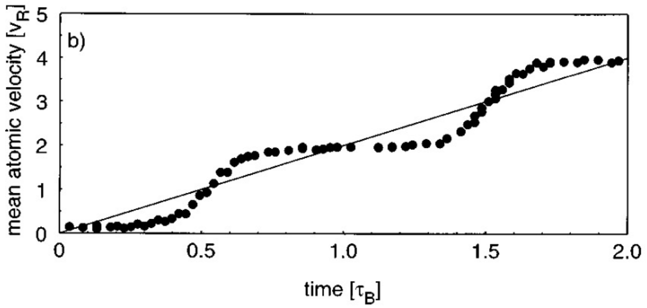

M. Ben Dahan, et al., Phys. Rev. Lett.76, 4508 (1996)
E. Peik, et al., Phys. Rev. A55, 2989 (1997),

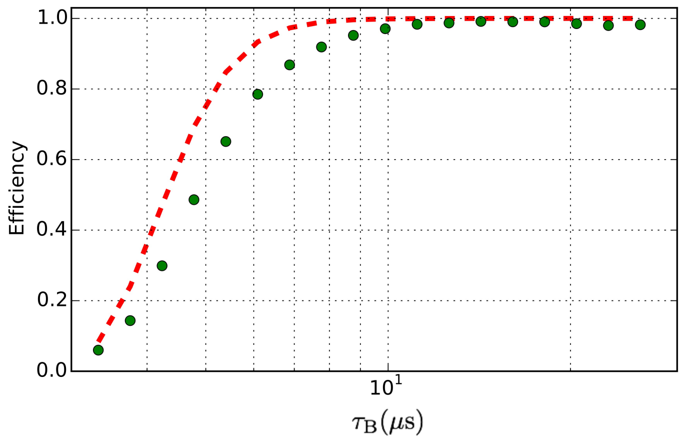

Experimental set-up

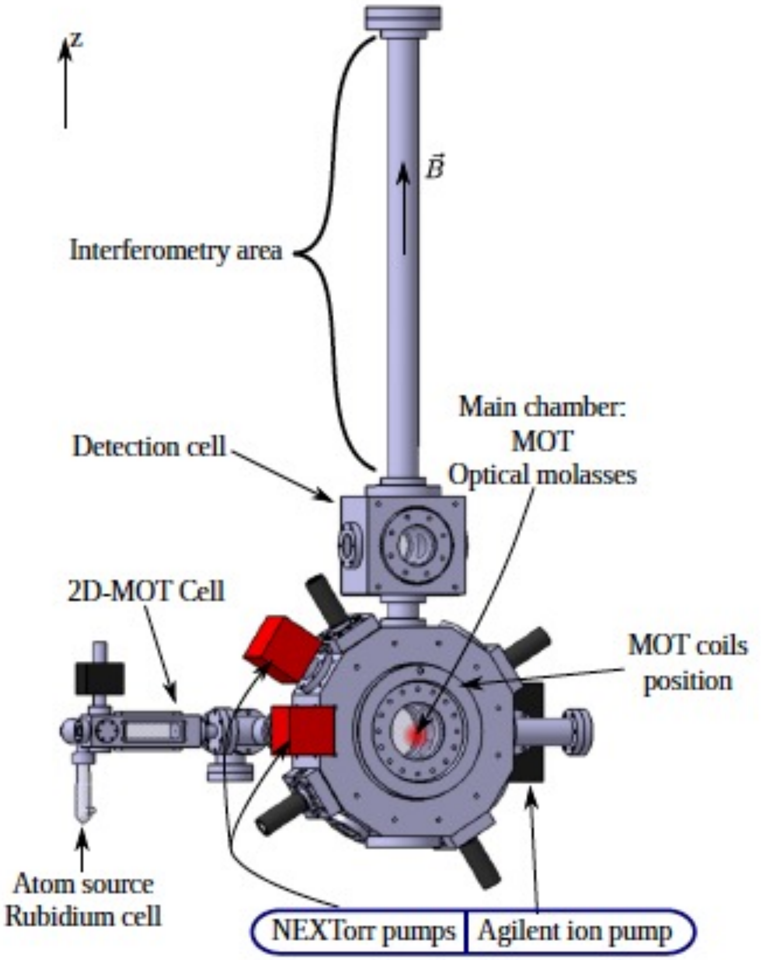

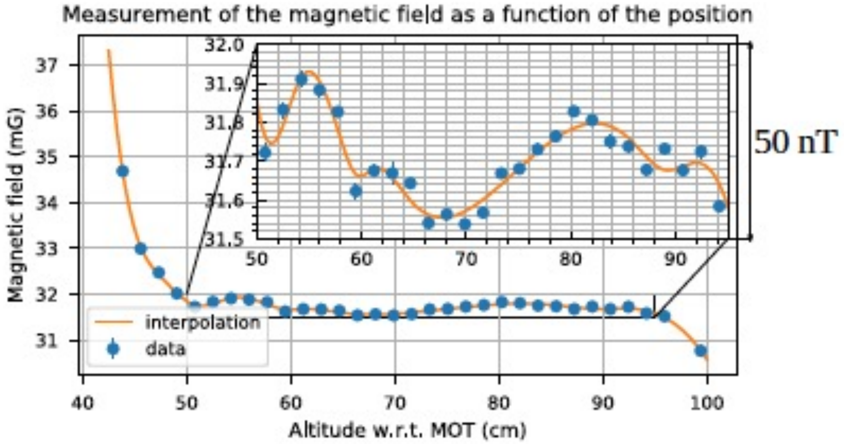

10^8 atoms ^{87}Rb : T=4 μK ; radius = 600 μm, 10^8 atoms

Phase and frequency control of Raman lasers

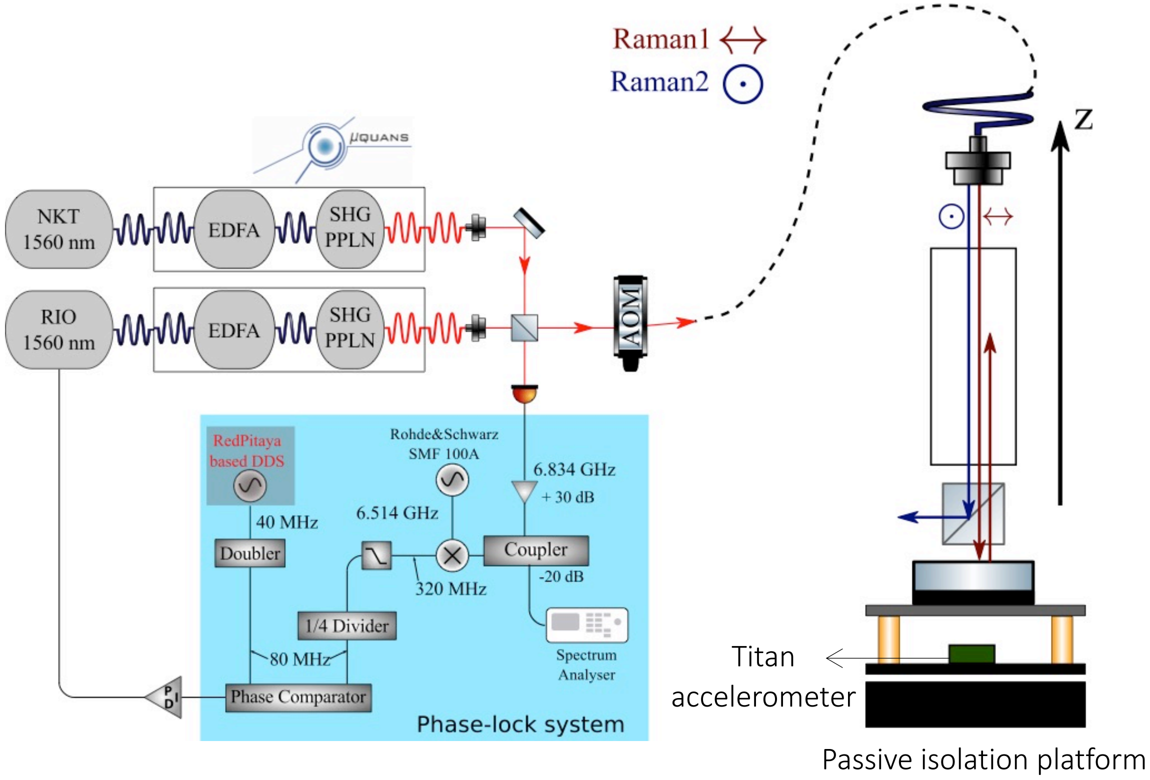

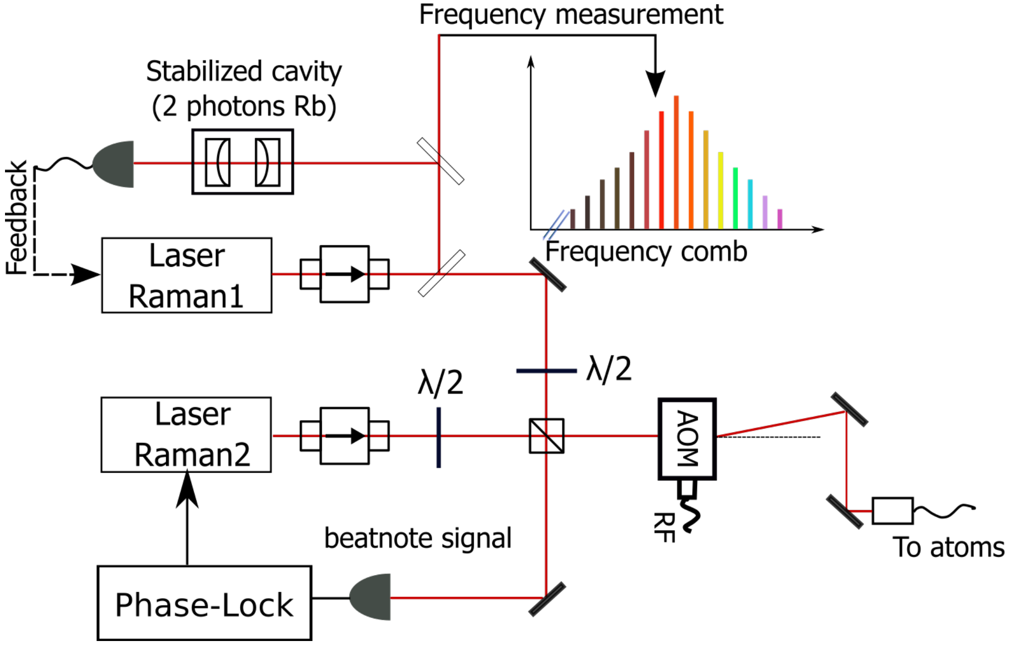

Frequency chain:

- Phase-lock of the two Raman lasers
- Frequency scanning during the second pair of $\pi/2$ pulses
- Frequency ramp to compensate for the Doppler shift during the free fall of atoms

Experiment principle

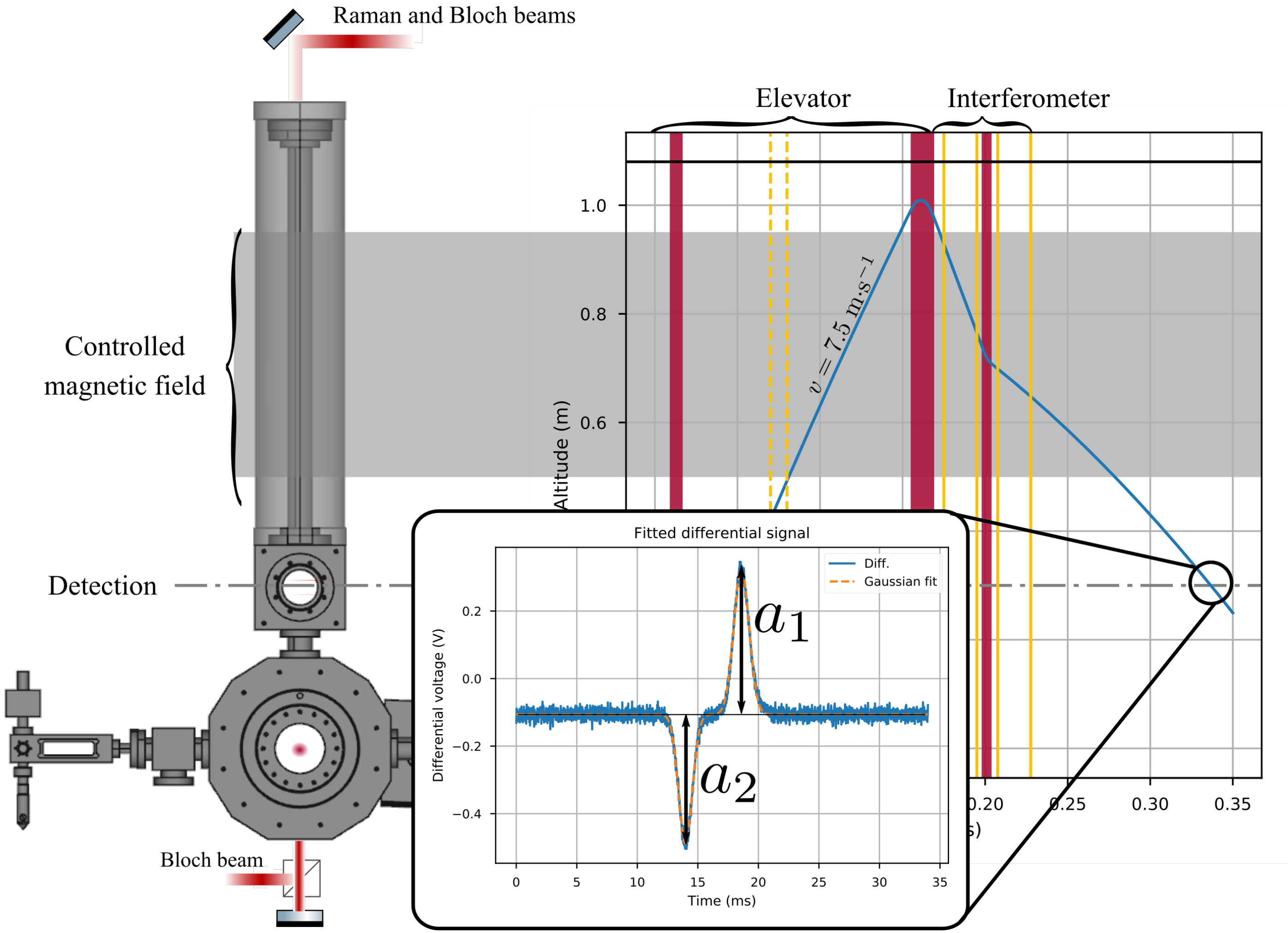

$$a_1 \propto N_1 \quad a_2 \propto N_2 \longrightarrow P_2 = \frac{N2}{N_1+N_2}$$

Typical atomic fringes

- T_{ramsey} = 20 ms, Number f Bloch oscillations N_B=500 (1000 v_r)
- 50 points per spectra in ~1 min

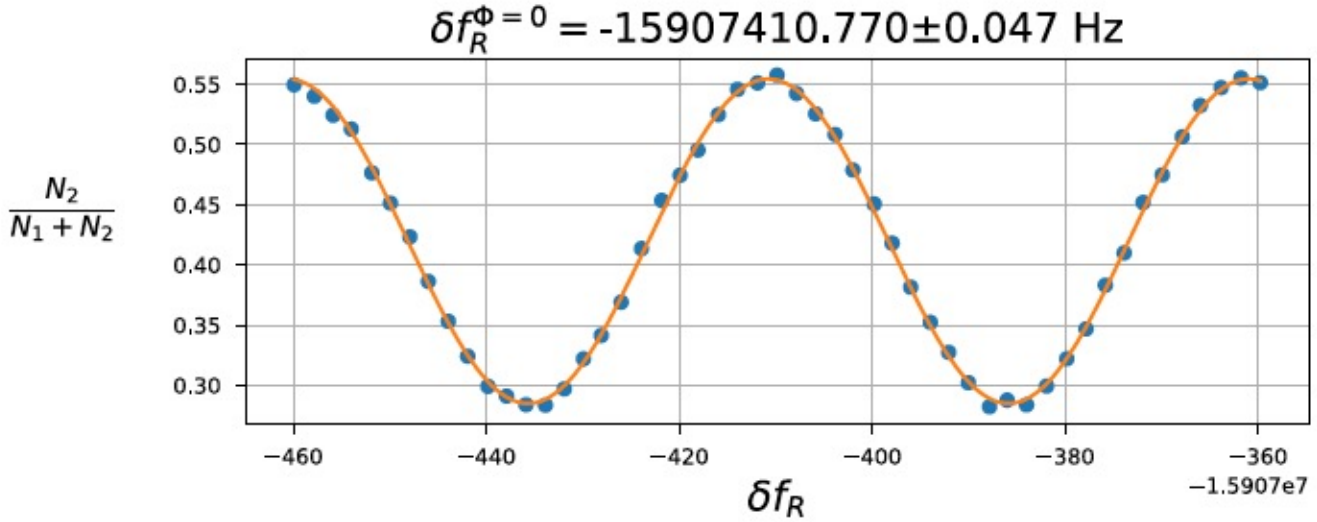

$$\Phi = T_{\mathrm{Ramsey}}\left(k_R\left(2N_B\frac{\hbar}{m}k_B - gT\right) - 2\pi\delta f_R\right) + \Phi^{LS}$$

- Recoil velocity (one photon momentum) ~ 15 kHz → 1000 v_r ~ 15 MHz
- σ_v=0.047 Hz ~ 3 x 10^{-6} v_r ~ 20 nm s^{-1} → 3 x 10^{-9} on h/m

➢ Contributions of g and the light shift Φ_{LS}

Measurement protocol

Four spectra in 4 minutes (200 points set arbitrary)

$$\Phi = T_{\mathrm{Ramsey}}\left(\epsilon_R k_R\left(\epsilon_B 2N_B \frac{\hbar}{m} k_B - gT\right) - 2\pi\delta f_R\right) + \Phi^{LS}, \text{ for } \epsilon_B = \pm 1,\ \epsilon_R = \pm 1$$

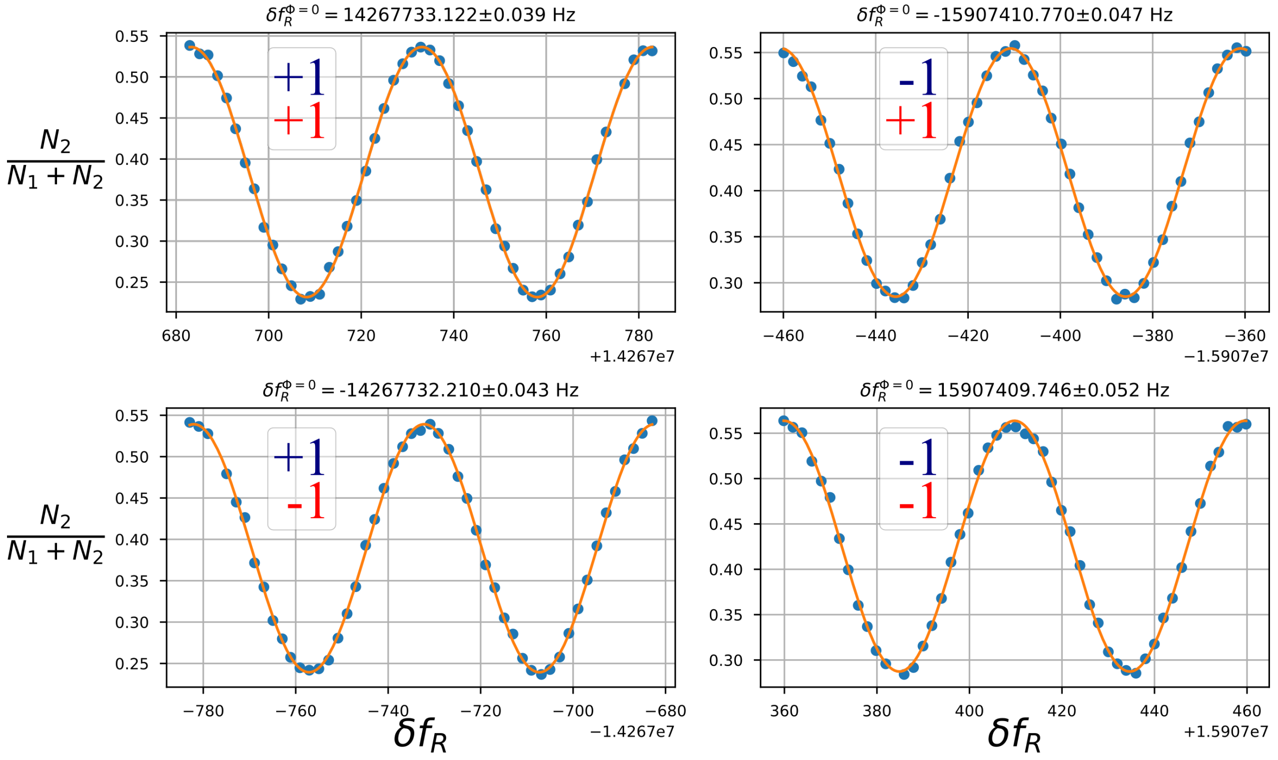

$$\frac{h}{m_{\mathrm{Rb}}} = \frac{2\pi^2}{N_B k_R k_B}\,\frac{1}{4}\sum_{4\ \mathrm{spectra}} \epsilon_R \epsilon_B \,\delta f_R^{\Phi=0}(\epsilon_R, \epsilon_B)$$

Laboratoire Kastler Brossel
Physique quantique et applications

Statistical uncertainty

Stable and reliable set-up: Long measurement period

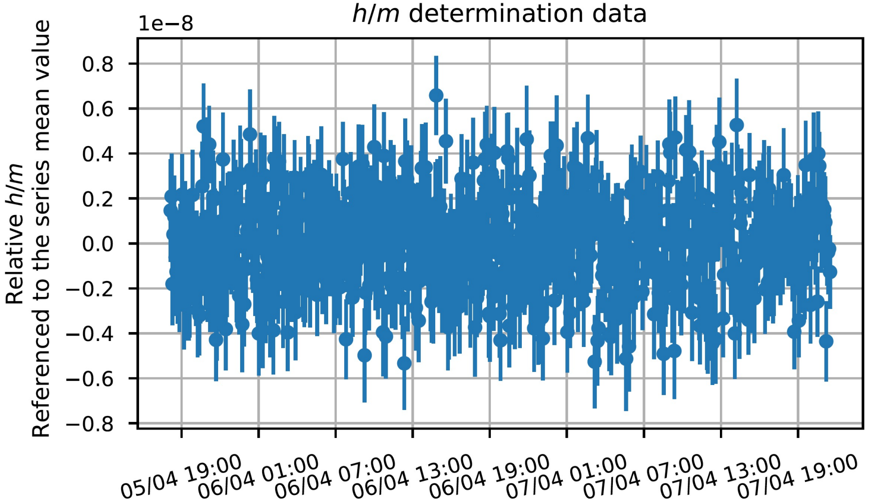

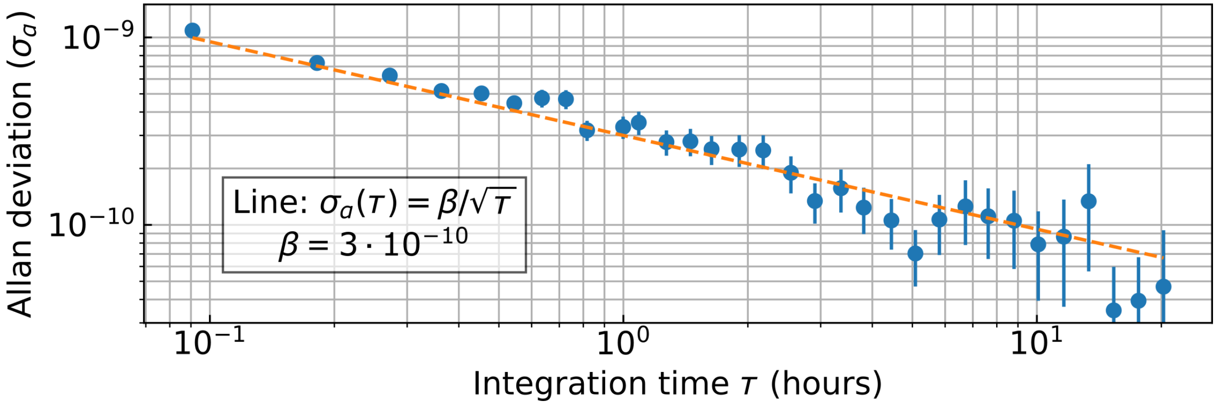

From Friday to .... Sunday

48 h integration: 8.5×10^{-11} on h/m $\longrightarrow$ 4.3×10^{-11} on α

Final data set (Jan. 2020)

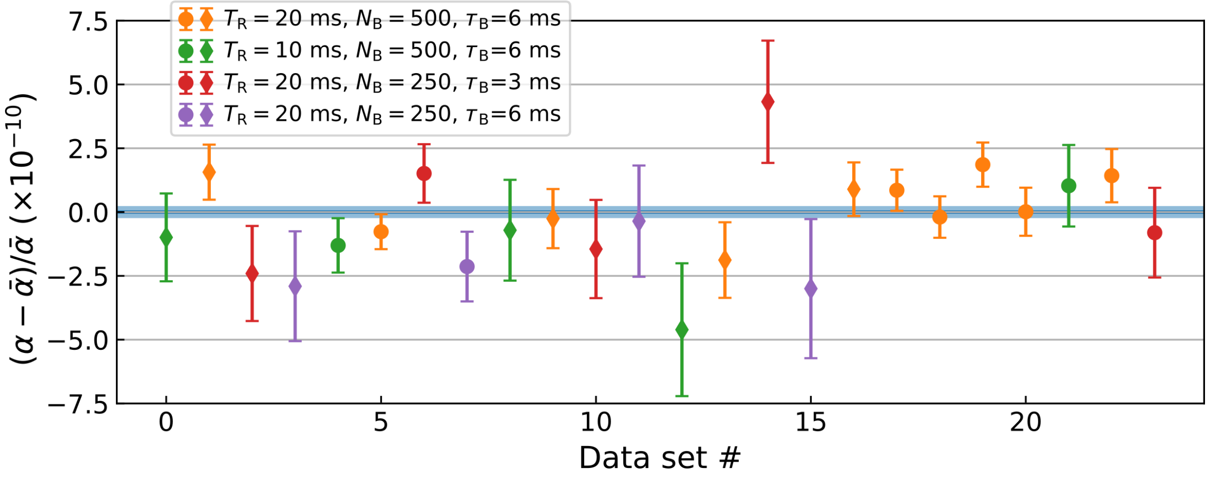

Error budget

Source	Correction $[10^{-11}]$	Relative uncertainty $[10^{-11}]$
Gravity gradient	-0.6	0.1
Alignment of the beams	0.5	0.5
Coriolis acceleration		1.2
Frequencies of the lasers		0.3
Wave front curvature	0.6	0.3
Wave front distortion	3.9	1.9
Gouy phase	108.2	5.4
Residual Raman phase shift	2.3	2.3
Index of refraction	0	< 0.1
Internal interaction	0	< 0.1
Light shift (two-photon transition)	-11.0	2.3
Second order Zeeman effect		0.1
Phase shifts in Raman phase lock loop	-39.8	0.6
Global systematic effects	64.2	6.8
Statistical uncertainty		2.4
Relative mass of ^{87}Rb [16] : $86.909\,180\,531\,0(60)$		3.5
Relative mass of the electron [14] : $5.485\,799\,090\,65(16) \cdot 10^{-4}$		1.5
Rydberg constant [14] : $10\,973\,731.568\,160(21)\mathrm{m}^{-1}$		0.1
Total: $\alpha^{-1} = 137.035\,999\,206(11)$		8.1

Atom recoil in a gaussian beam

- Electric field: $E(\vec{r},t) = A(\vec{r},t)\ \mathrm{e}^{i\phi(\vec{r})} \longrightarrow \vec{k}_{\mathrm{eff}} = \vec{\nabla}\phi(\vec{r})$
- Plane wave model: $k = \frac{\nu}{c}$
- Gaussian laser beam correction: $k_{\mathrm{eff},z} = k + \delta k$

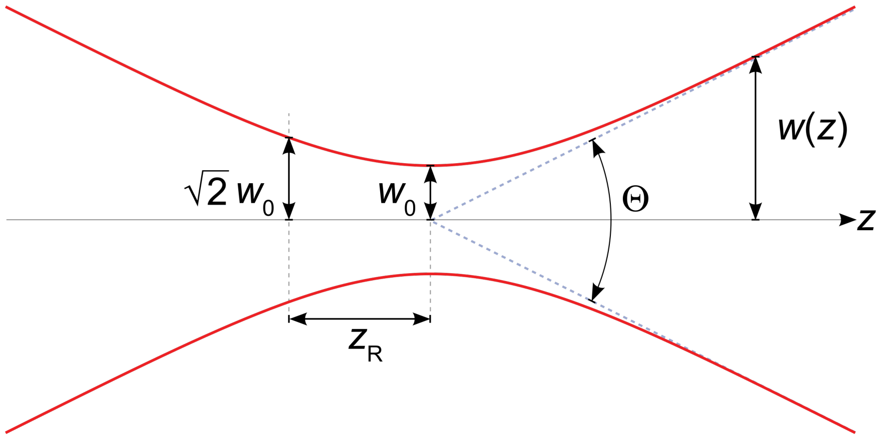

$$\frac{\delta k}{k} = -\frac{2}{k^2 w^2(z)}\left(1 - \frac{\langle r^2\rangle}{w^2(z)}\right) - \frac{\langle r^2\rangle}{2R^2(z)}$$

Size of the atomic cloud

Curvature of the wavefront

- Related to the dispersion of wavevectors $\sim \dfrac{\Theta^2}{2}$

Recoil velocity of atom in a distorted wave front

- A systematic effect that depends on the efficiency of the Bloch oscillation

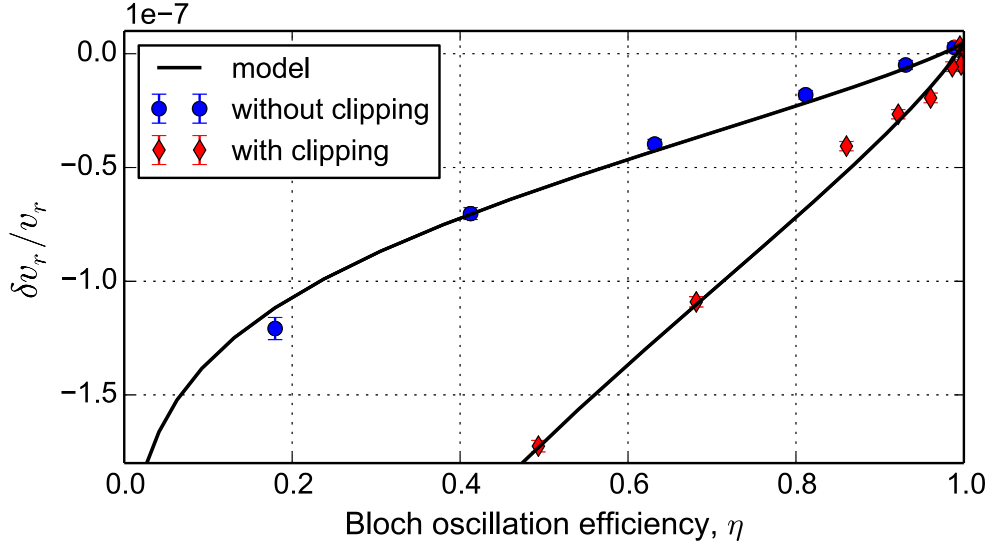

- During the Bloch Oscillation pulse, the survival probability is governed by Landau-Zener Losses, it depends on laser intensity

Recoil velocity of atom in a distorted wave front

- Electric field: $E(\vec{r},t) = A(\vec{r},t)\ \mathrm{e}^{i\phi(\vec{r})}$

Random spatial fluctuations of laser intensity with typical correlation length 100 μm

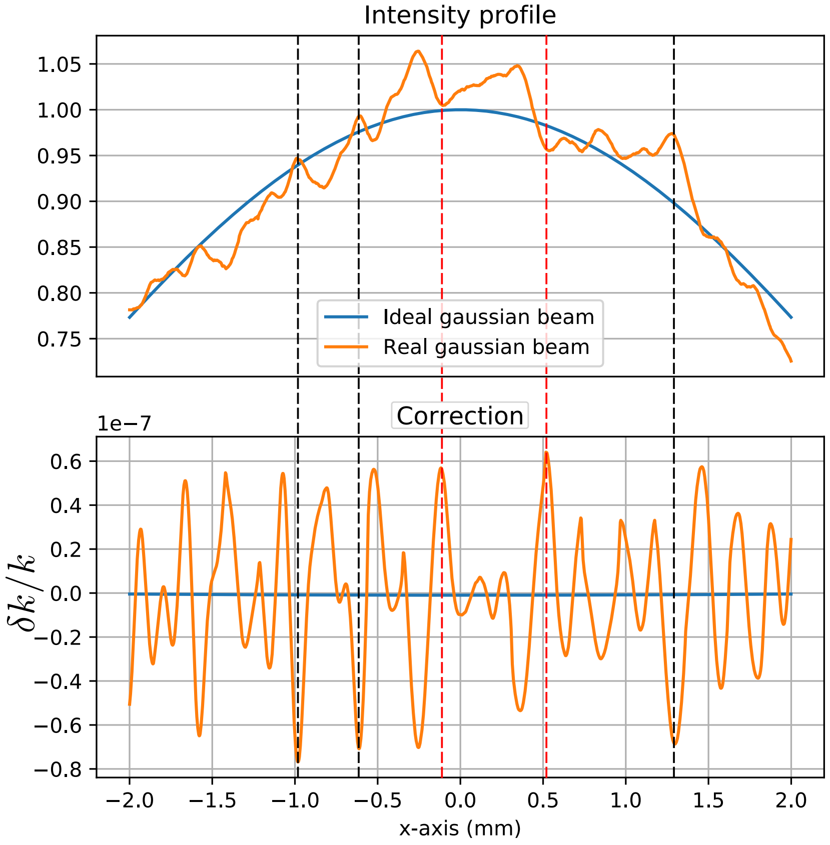

$$k_{\mathrm{eff},z} = \frac{\partial \phi}{\partial z} = k + \delta k$$

Local amplitude fluctuations induces momentum correction (in paraxial approximation)

$$\frac{\delta k}{k} = -\frac{1}{2}\left\|\frac{\vec{\nabla}_\perp \phi}{k}\right\|^2 + \frac{1}{2k^2}\frac{\triangle_\perp A}{A}$$

Correlation between the wave vector correction and the survival probability *P*(I) during Bloch oscillations,

$$\langle \delta k \rangle = \frac{\langle \delta k\ P(I)\rangle}{\langle P(I)\rangle}$$

Observation of extra photon recoil in a distorted optical field

S. Bade, L. Djadaojee, M. Andia, P. Cladé, and S. Guellati-Khelifa, Phys. Rev. Lett 121 073603 (2018)

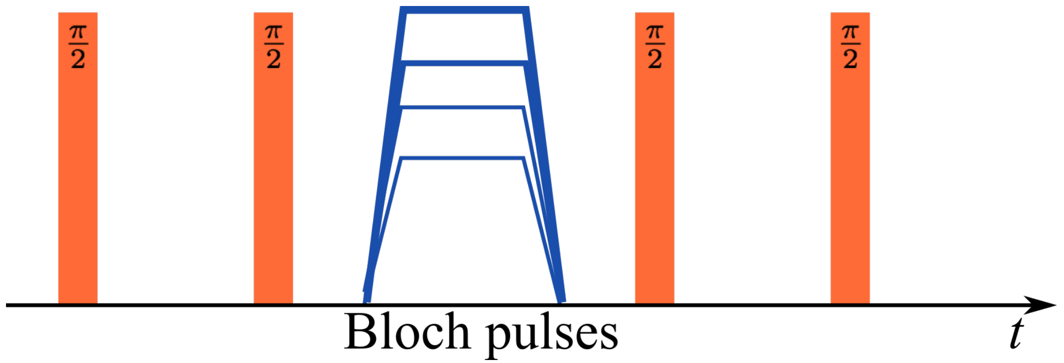

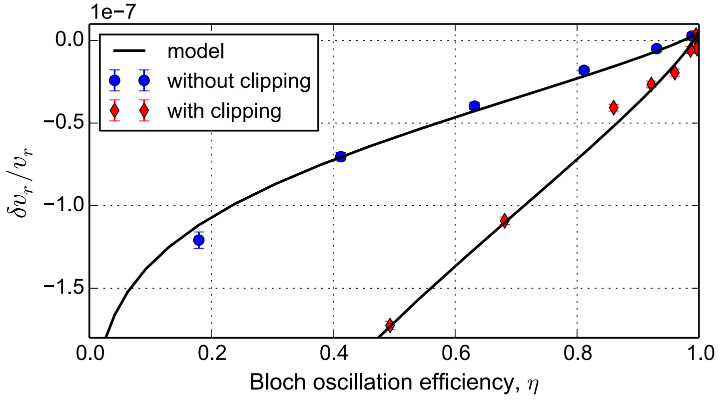

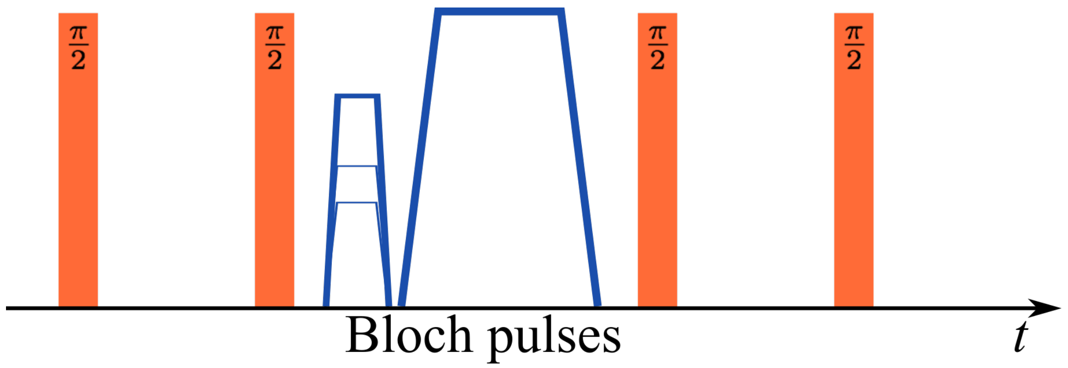

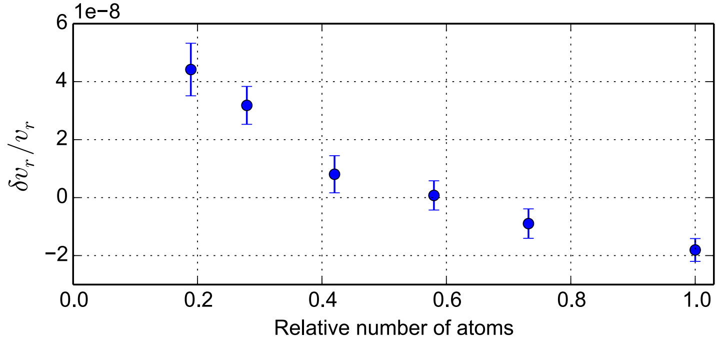

- The momentum of a photon can be locally higher than $\frac{h\nu}{c}$!
- Better understandig of local photon momentun, this model replaces the usual Gouy phase correction.

Recoil velocity of atom in a distorted wave front

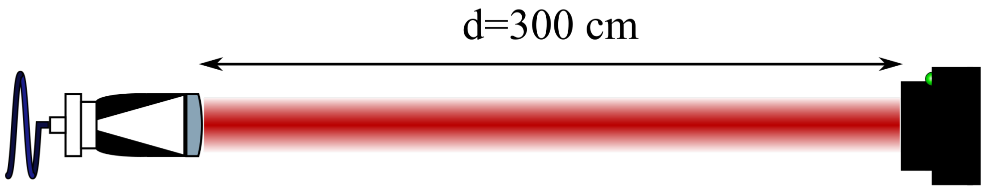

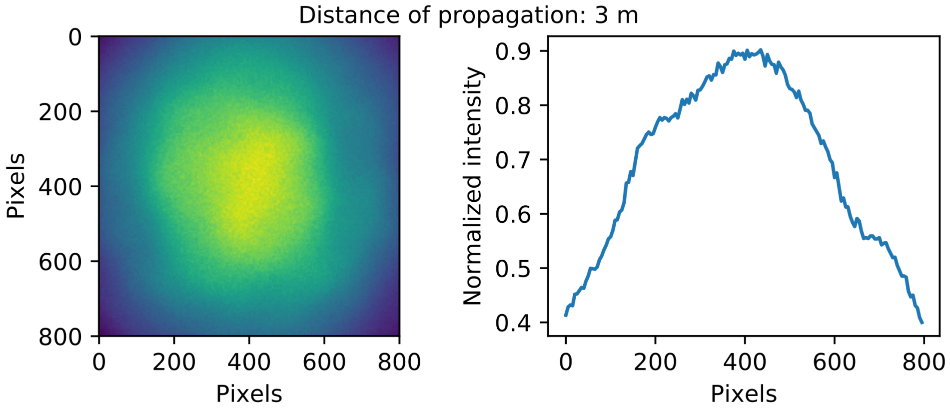

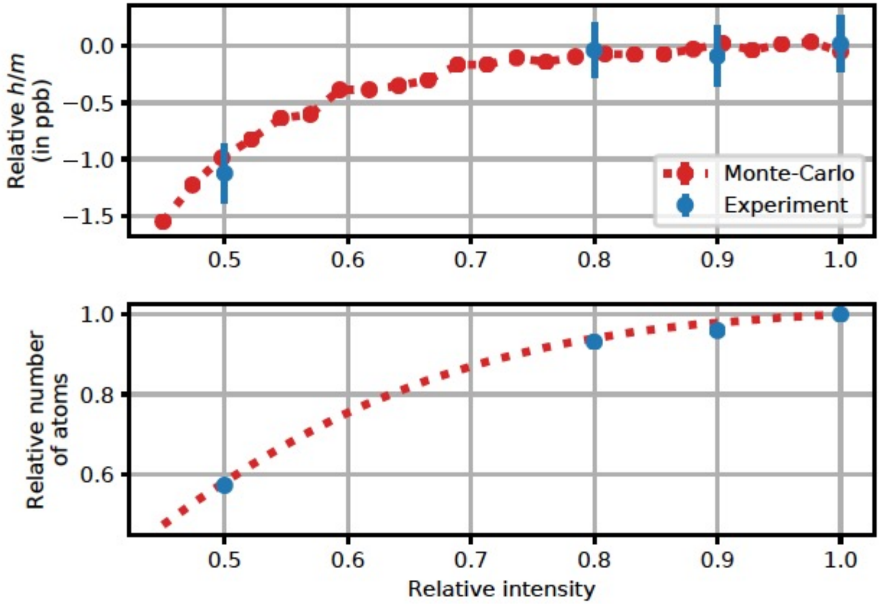

Effect on α: $(3.9 \pm 1.9)\times 10^{-11}$

Outline

Laboratoire Kastler Brossel
Physique quantique et applications

- Measurement of the ratio *h*/*M*
- Impact of the new determination of the fine-structure constant

Recent results

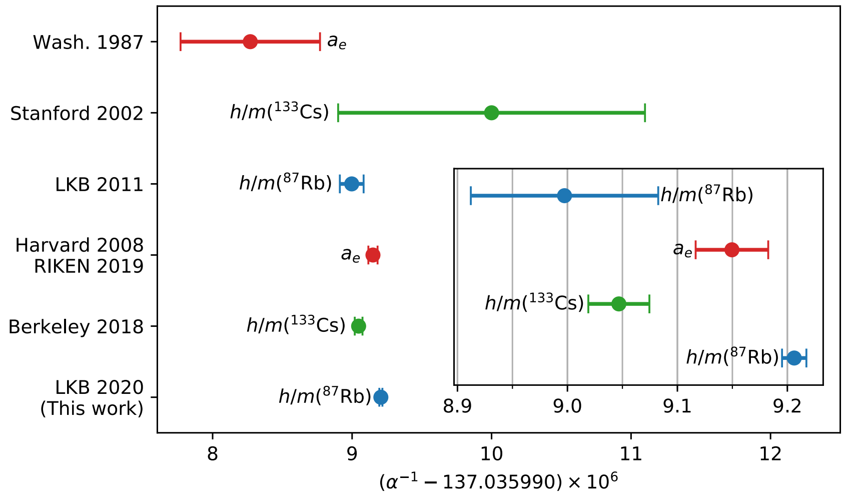

$$\alpha^{-1} = 137.035999206(11)$$

- Statistical uncertainty of 4.3×10^{-11} on 48h integration time
- New systematic effects were considered
- 5.4 σ discrepancy with cesium recoil measurement

R. H. Parker et al., Scie,ce 360, 191-195 (2018)
L. Morel et al., Nature 588, 61-68 (2020)

$$a_e(\exp) - a_e(\alpha_{\mathrm{LKB2020}}) = (4.8 \pm 3.0) \times 10^{-13} \quad (+1.6\sigma)$$
$$a_e(\exp) - a_e(\alpha_{\mathrm{Berkeley}}) = (-8.8 \pm 3.6) \times 10^{-13} (-2.6\sigma)$$

- The uncertainty on δa_e is now dominated by $a_e(\exp)$

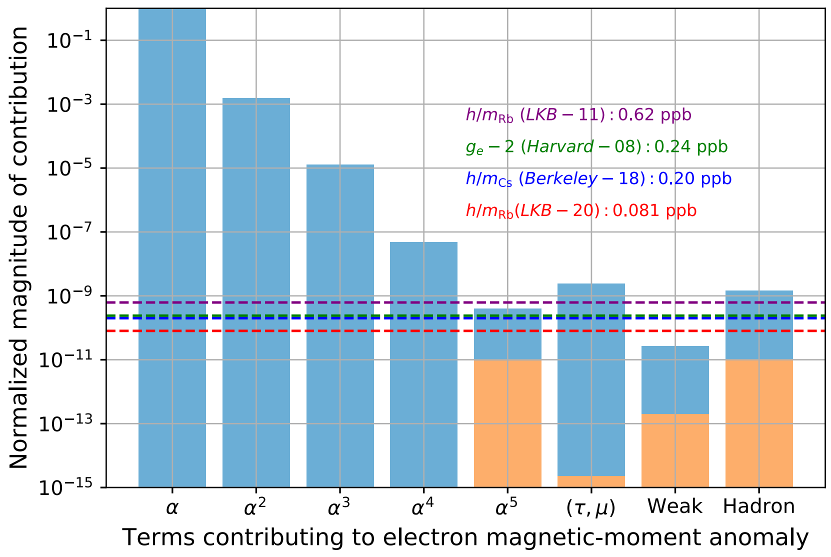

Testing the muon a_μ discrepancy in the electron sector

$$\delta a_\mu = a_\mu(\mathrm{exp}) - a_\mu(\mathrm{theo}) = 250\ (0.86)^{-9}\ (3.4\sigma)$$

- Recent re-evaluation of theoretical value confirmed the discrepancy

T. Aoyama et al., Physics Reports 887, 1-66 (2020)

- Naive scaling $$\left|\frac{\delta a_\mathrm{e}}{\delta a_\mu}\right| = \left(\frac{m_\mathrm{e}}{m_\mu}\right)^2 \simeq 2.3\times10^{-5} \implies \sigma_{a_\mathrm{e}} = 2.5\times10^{-9}\times\left(\frac{m_\mathrm{e}}{m_\mu}\right)^2 \simeq 5.8\times10^{-14}$$

F. Terranova and G. M. Tino, PRA 89, 052118 (2014)

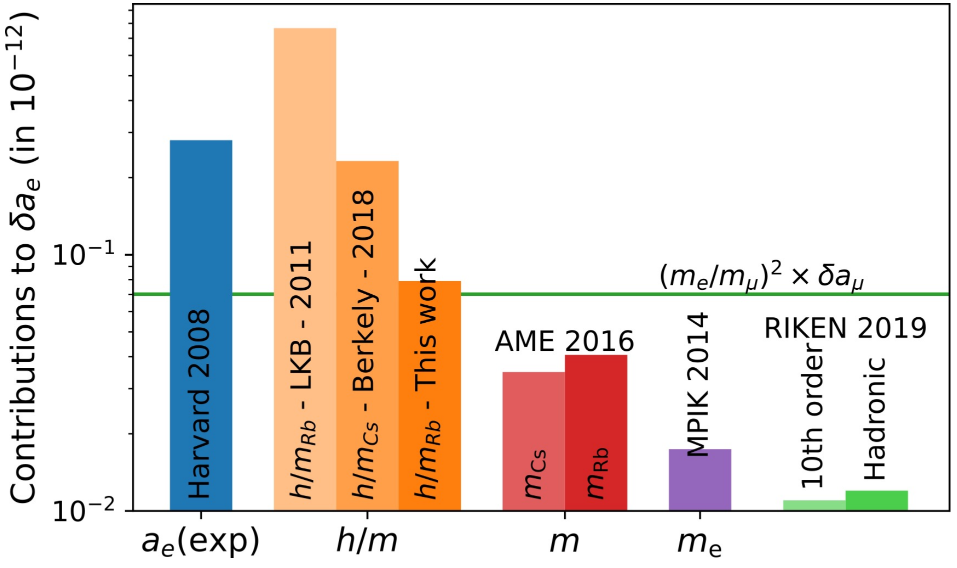

Physics beyond Standard Model

« Hypothetical particles » of mass m_V and coupling ε with electrons will induce

$$\delta a_e = \frac{\alpha}{\pi} \times \epsilon^2 \int_0^1 dz \frac{2m_e^2 z(1-z)^2}{m_e^2(1-z)^2 + m_V^2 z} \simeq \frac{\alpha\epsilon^2}{3\pi}\frac{m_e^2}{m_V^2} \quad \text{For} \quad m_V \gg m_e$$

Our results rejects with 95% confidence level $\delta a_e > 9.8 \times 10^{-13}$ and $\delta a_e < -3.4 \times 10^{-13}$

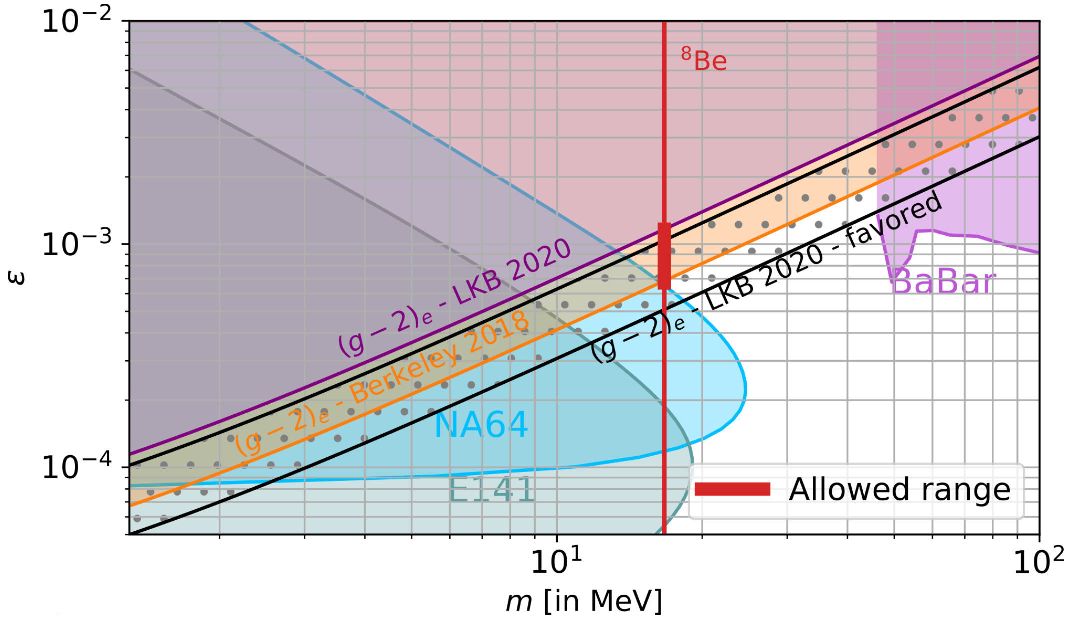

D. Banerjee et al. (The NA64 Collaboration) Phys. Rev. D 101, 071101(R) (2020)

- Favoured the hypothetical X(16.7 MeV) boson that could explain the anomalous excess of e^+e^- pairs observed in the decays of the excited ^{8}Be∗ nuclei (“Beryllium or X17 anomaly”)

A. J. Krasznahorkay et al., Phys. Rev. Lett. 116, 042501 (2016)

New international System of units

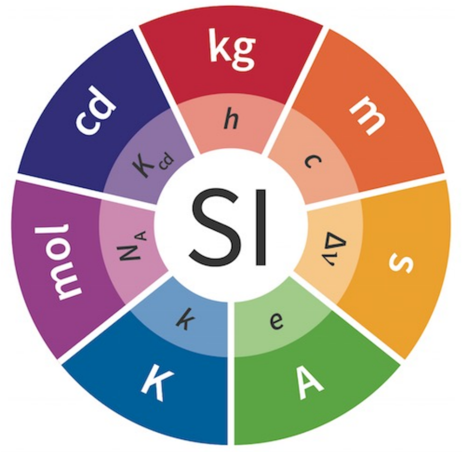

- The new SI (since 20 may 2019)
  Based on fundamental constants $\Delta\nu_{Cs}$, *c*, *h*, *e*, N_A, K_{cd}

- Our experiment allow the *Mise en pratique* of the new kilogramme at the atomic scale

$$m(^{87}\mathrm{Rb}) = 1.44316089776\ (21)\ \times 10^{-25}\ \mathrm{kg}$$

- The Avogadro constant N_A is also fixed for new definition of the mole, molar mass of carbon-12 will no longer be exactly defined

$$M(^{12}\mathrm{C}) = N_A \times m(^{12}\mathrm{C}) = \frac{12 N_A h}{h/m_\mathrm{u}} = 12.0000000173(19)\ \mathrm{g/mol} \quad \text{where} \quad m_\mathrm{u} = \frac{m_\mathrm{X}}{A_\mathrm{r}(\mathrm{X})}$$

- The fine-structure constant plays an important role in the adjustment of fundamental physical constants:
  in the new SI the numerical values of ε_0 et μ_0 will depend on a.

$$\mu_0 = \frac{2\alpha h}{e^2 c} = 0.999999999648(80) \times 4\pi \times 10^{-7}\ \mathrm{m}\cdot\mathrm{kg}\cdot\mathrm{s}^{-2}\cdot\mathrm{A}^{-2}$$

90 of the 354 constants listed by NIST (https://physics.nist.gov/cuu/Constants/) will have their uncertainties reduced.

Conclusion and prospects

- New determination of the fine-structure constant with a relative uncertainty of 8.11×10^{-11}
- The sensitivity of the experimental set-up allowed the experimental investigation of several systematic effects,
- Three new systematic effects were identified
- The large disagreement ($5.4\ \sigma$) with the cesium measurement needs to be clarified

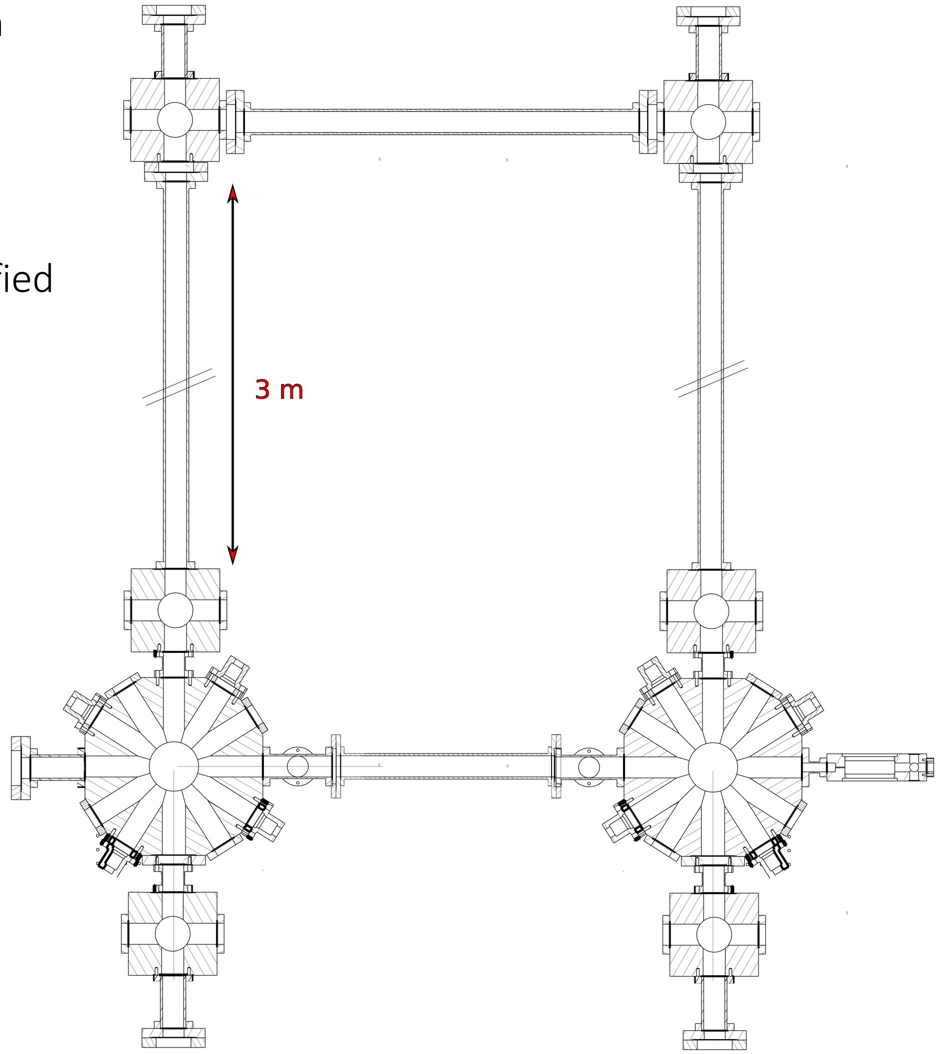

Prospects:

- New measurement using ultra-cold atoms is in progress (Bose-Einstein condensate)
- Measurement of recoil velocity with rubidium isotope 85
- New experimental setup : uncertainty on α of 10^{-11}

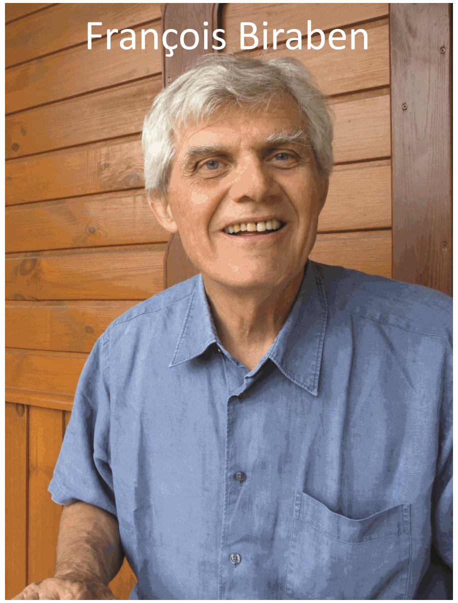

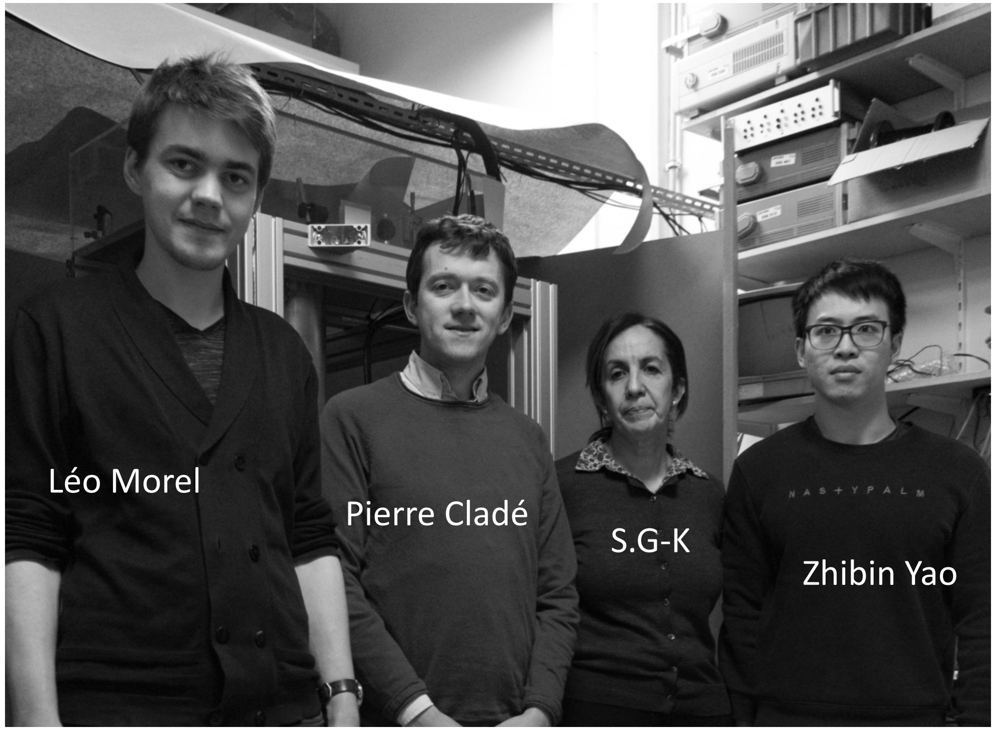

PhD students (since 2000):

- L. Morel
- Z. Yao
- M. Andia
- R. Jannin
- C. Courvoisier
- R. Bouchendira
- M. Cadoret
- P. Cladé
- R. Battesti

Thank you !

PROJET FINANCÉ PAR L'ANR - PROJECT FUNDED BY THE ANR
ANR
NIST
National Institute of Standards and Technology
U.S. Department of Commerce
DEPARTMENT OF JUSTICE
FEDERAL BUREAU OF INVESTIGATION
DGA
Liberté • Égalité • Fraternité
RÉPUBLIQUE FRANÇAISE
MINISTÈRE DE LA DÉFENSE
Institut Francilien de Recherche sur les Atomes Froids
IFRAF